Transverse correlation in optical spontaneous parametric down-conversion

Morton H. Rubin
Department of Physics, University of Maryland Baltimore County, Baltimore, Maryland 21228-5398
(Received 5 June 1996; revised manuscript received 12 August 1996)

The transverse correlation between the pairs of photons produced in optical spontaneous parametric down-conversion is analyzed. The interesting features of the correlation arise from the form of the two-photon state generated in the process. The physics of the rings of radiation emerging from the crystal is described. We discuss the theory behind the recent experiments on two-photon geometric and physical optics. [S1050-2947(96)03812-7]

PACS number(s): 42.50.Dv, 03.65.Bz

I. INTRODUCTION

The correlated photon pairs produced in optical spontaneous parametric down-conversion (SPDC) have many interesting properties. To date most experiments have concentrated on the effect of the frequency phase matching. Early experiments to study the spatial correlations were performed by Penin and co-workers [1], and interesting focusing effects were predicted by Klyshko [2,3]. Theoretical and experimental studies of the polarization and frequency correlation of type-II SPDC have been published [4–8]. In this paper we present a theoretical treatment of the transverse correlations in SPDC with emphasis on the geometrical and physical optics properties of the two-photon amplitude or biphoton. In addition we study the coherence of the individual beams. The experiment of Zou, Wang, and Mandel [9] has led to some discussion [10] of the effect of transverse correlation on coincidence counting rates. Recent experiments have illustrated some of the interesting effects of the transverse correlations in image transfer experiments [11–13]. A discussion on the second order and fourth order coherence functions and the effects of the pulse shape of the pump beam on the transverse correlations has been published [14]. Our paper complements that work in that we emphasize the nature of the biphoton or two-photon amplitude and its role in the experiments cited above.

The quantity that must be calculated carefully is the spectral function of the two-photon state, F, which has been extensively studied by Klyshko [15]. The imaging properties are determined by the transfer function of the passive, linear optical systems placed in front of the detectors and by F. The novel properties of this system are determined by F. SPDC is a coherent effect in which a pump laser drives the atomic oscillators in a noncentrosymmetric crystal into the nonlinear regime. The down-converted beams are in turn radiated by these oscillations. The beams which emerge from the crystal must be phase matched with the pump over the entire crystal. In the analysis of F this phase matching emerges naturally. We present a detailed study of the phase matching using the beam invariants of frequency and transverse wave number. One result of this shows how the frequency and wave number phase matching interlock the spatial and temporal transverse coherence.

II. CLASSICAL OPTICS

We first show how the single and coincident counting rates are determined by F and the linear optical systems placed between the down-converting crystal and the detectors. Consider the experiments illustrated in Fig. 1. A monochromatic laser beam incident on a noncentrosymmetric birefringent crystal produces pairs of photons by SPDC. Each beam is transmitted through a linear optical system which may include pinholes, lenses, beam splitters, and polarization manipulators. The photons are detected by point photodetectors and both the single counts and coincidence counts are recorded. The system is arranged so that only one pair of photons at a time can be detected. In Fig. 1(a) each beam is sent to one detector, while in Fig. 1(b) each photon may go to either detector. We shall concentrate on case (a), the generalization to (b) is straightforward.

The average coincidence counting rate is defined by

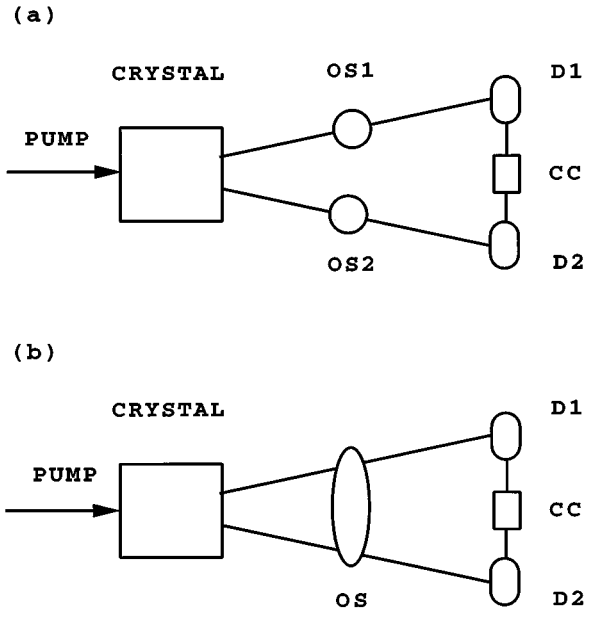

FIG. 1. The OS's are passive linear optical systems, $D1$ and $D2$ are point photodetectors, and CC is a coincidence counter. The beams are not mixed in the optical system illustrated in (a). The optical system in (b) contains beam splitters that mix the beams.

$$R_c = \lim_{T\to\infty}\frac{1}{T}\int_0^T dt_1\int_0^T dt_2\langle\Psi|E_1^{(-)}E_2^{(-)}E_2^{(+)}E_1^{(+)}|\Psi\rangle, \quad (1)$$

and the counting rate at detector 1 is given by

$$R_1 = \lim_{T\to\infty}\frac{1}{T}\int_0^T dt_1\langle\Psi|E_1^{(+)}E_1^{(+)}|\Psi\rangle. \quad (2)$$

The field $E_j^{(+)}$ is the positive frequency part of the electric field evaluated at the position $\mathbf{r}_j$ and the time t_j and $E_j^{(-)}$ is its Hermitian adjoint. These are free space fields defined by

$$E_1^{(+)} = \sum_{\mathbf{k}} e_{\boldsymbol{\omega}} b_{\mathbf{k}\beta} e^{i(\mathbf{k}\cdot\mathbf{r}_1-\omega t_1)}, \quad (3)$$

$$e_{\boldsymbol{\omega}} = \sqrt{\frac{\hbar\omega}{2\epsilon_0 V}}, \quad (4)$$

where $|\mathbf{k}| = \omega/c, b_{\mathbf{k}\beta}$ is the destruction operator at detector 1 for a photon with polarization β and wave-number $\mathbf{k}$, and V is the quantization volume. Ψ is the state of the system at the output face of the crystal [4]. In general, Ψ will be a superposition of the vacuum state $|0\rangle$ and states with any number of pairs of photons. We ignore the pump which is blocked and does not affect the counting rates. Because the nonlinearity in the crystal is small, the expansion of Ψ may be limited to two terms,

$$|\Psi\rangle = |0\rangle + \sum_{\mathbf{k},\mathbf{k}'} F(\mathbf{k}\beta,\mathbf{k}'\beta')a^\dagger_{\mathbf{k}\beta}a^\dagger_{\mathbf{k}'\beta'}|0\rangle, \quad (5)$$

where $\mathbf{k}$ and $\mathbf{k}'$ are evaluated inside the crystal and $a^\dagger_{\mathbf{k}\beta}$ is the creation operator at the surface of the crystal.

For type-I down-conversion β and β' are both ordinary rays (o rays) or extraordinary rays (e rays), while for type II one is an o ray and the other is an e ray. We shall use the convention of referring to the beam corresponding to the first index in F as the signal and the second as the idler.

Using Eq. (5), the fourth order correlation function reduces to

$$\langle\Psi|E_1^{(-)}E_2^{(-)}E_2^{(+)}E_1^{(+)}|\Psi\rangle = |A_{12}|^2, \quad (6)$$

where

$$A_{12} = \langle 0|E_2^{(+)}E_1^{(+)}|\Psi\rangle \quad (7)$$

is the two-photon amplitude or biphoton [4,15]. The second order correlation function may be written as

$$\langle\Psi|E_1^{(-)}E_1^{(+)}|\Psi\rangle = \sum_{\mathbf{k},\beta}|\langle 0|a_{\mathbf{k}\beta}E_1^{(+)}|\Psi\rangle|^2. \quad (8)$$

The electric field for the beam at detector 1, E_1, can be written in terms of the electric field on the output surface of the crystal using the Green's function G which describes the propagation of the beam through the optical system,

$$E_1 = \sum_{\mathbf{k},\beta} G_{1,\mathbf{k}\beta}E_{\mathbf{k}\beta}. \quad (9)$$

A similar expression exists for detector 2. For the experiment illustrated in Fig. 1(a), the biphoton at the detectors is calculated in terms of the biphoton on the crystal surface by

$$A_{12} = \sum_{\mathbf{k}\beta,\mathbf{k}'\beta'} G_{1,\mathbf{k}\beta}G_{2,\mathbf{k}'\beta'}A_{\mathbf{k}\beta,\mathbf{k}'\beta'}, \quad (10)$$

where

$$A_{\mathbf{k}\beta,\mathbf{k}'\beta'} = e_{\boldsymbol{\omega}}e_{\boldsymbol{\omega}'}F(\mathbf{k}\beta,\mathbf{k}'\beta') \quad (11)$$

and F, the spectral representation of the biphoton obtained from Eq. (5), is defined by

$$F(\mathbf{k}\beta,\mathbf{k}'\beta') = \langle 0|a_{\mathbf{k}\beta}a_{\mathbf{k}'\beta'}|\Psi\rangle. \quad (12)$$

For Fig. 1(b), a term containing $G_{1,\mathbf{k}'\beta'}G_{2,\mathbf{k}\beta}$ must be included in (10).

If only the idler reaches detector 1,

$$\langle 0|a_{\mathbf{k}\beta}E_1^{(+)}|\Psi\rangle = \sum_{\mathbf{k}'\beta'} G_{1,\mathbf{k}'\beta'}e_{\boldsymbol{\omega}'}F(\mathbf{k}\beta,\mathbf{k}'\beta'). \quad (13)$$

To evaluate the sums over the wave numbers, we must be careful to note that the wave numbers in F are evaluated inside the crystal and those at the detector are evaluated in free space. It is simplest to work with the quantities that are invariant along the beam: ω, the angular frequency, and $\boldsymbol{\kappa}$, the component of the wave number parallel to the output face of the crystal. Then the z component of the wave number for a photon with polarization β is

$$k_z = \sqrt{\left(\frac{\omega n_\beta(\omega)}{c}\right)^2 - \boldsymbol{\kappa}^2}. \quad (14)$$

Outside the crystal, the index of refraction $n_\beta(\omega) = 1$. For e rays inside the crystal, n_e will depend on the angle between the optic axis of the crystal and the wave vector of the beam [16].

In general, the Green's function $G_{1,\mathbf{k}\beta}$ will depend on the transverse coordinate of detector one, $\boldsymbol{\rho}_1$, the distance from the surface of the crystal to the plane of the detector, z_1, and the time t_1, when detector 1 fires. Consequently,

$$G_{1,\mathbf{k}\beta} = e^{-i\omega t_1}g_1(\boldsymbol{\kappa},\omega,\boldsymbol{\rho}_1,z_1)d_{\mu_1\beta}, \quad (15)$$

where the index μ_1 signifies the component of the polarization that the detector registers and $d_{\mu_1\beta}$ is the polarization transfer function [4]. The function g, which depends on the details of the optical system, is discussed in Appendix A.

Finally, we have

$$A_{12} = \sum_{\mathbf{k}_1}\sum_{\mathbf{k}_2} e^{-i(\omega_1 t_1+\omega_2 t_2)}e_{\omega_1}e_{\omega_2}d_{\mu_1\beta_1}d_{\mu_2\beta_2} \times \sum_{\beta_1,\beta_2} g_1(\boldsymbol{\kappa}_1,\omega_1,\boldsymbol{\rho}_1,z_1) \times g_2(\boldsymbol{\kappa}_2,\omega_2,\boldsymbol{\rho}_2,z_2)F(\mathbf{k}_1\beta_1,\mathbf{k}_2\beta_2) \quad (16)$$

and

$$\langle 0|a_{\mathbf{k}\beta}E_1^{(+)}|\Psi\rangle=\sum_{\mathbf{k}_1\beta_1} e^{-i\omega_1 t_1}g_1(\boldsymbol{\kappa}_1,\omega_1,\boldsymbol{\rho}_1 z_1) \times d_{\mu_1\beta_1}e_{\boldsymbol{\omega}_1}F(\mathbf{k}\beta,\mathbf{k}_1\beta_1). \quad (17)$$

Equations (16) and (17) show that the counting rates are determined by classical optical transfer functions and the biphoton spectral function F.

Klyshko has noted that these formulas can be interpreted in terms of single-photon optics using an advanced wave picture in which one of the photons is generated at one detector, propagates backwards in time to the crystal where it turns into the second photon, and then propagates forward in time to the other detector [17,18]. The crystal behaves like a nonlinear mirror since it can change the wavelength of the ''reflected'' light.

Using this picture, detector 2 can be thought of as a source emitting waves at $(\boldsymbol{\rho}_2,z_2)$ and transmitting them to detector 1 at $(\boldsymbol{\rho}_1,z_1)$. In Eq. (16) detector 2 acts as a coherent point source. The advanced wave picture can be used for the singles counting rate, also. Equation (17) shows that the effective source of the waves reaching detector 1 is an incoherent plane wave source which emits radiation over a large frequency range into a large solid angle. Because this effective source is incoherent, when (17) is substituted into (8) all phase information between the different $\mathbf{k}$ in F is lost.

There is another interpretation of Eq. (7) in terms of spatial modes of the electromagnetic field. Instead of expressing Fin terms of plane waves, we can express it in terms of some other set of modes U_n and V_n as $F=\Sigma_n c_n U_n^{(s)}V_n^{(i)}$. The important point is that the modes of the signal and idler are correlated or entangled so that F does not factor into a function describing the signal times a function describing the idler. The optical system can then be thought of as projecting out a subset of these modes. In the case that the signal and idler beams are not mixed one can interpret the counting rate in terms of the type of experiments using preselected and postselected states discussed in [19]. Suppose the idler is detected first, from this we can infer the state of the signal at that time and then choose to measure its projection onto another state at a later time.

III. THE SPECTRAL REPRESENTATION OF THE BIPHOTON

We have presented the calculation of the quantity F defined in Eq. (12) elsewhere [4,13]. We summarize the results of those calculations. The state Ψ is computed using the standard down-conversion Hamiltonian [15,20] and first order perturbation theory. Assuming that the pump is a classical steady-state monochromatic wave, it is not difficult to show that

$$F(\mathbf{k}\beta,\mathbf{k}'\beta')=\Gamma\,\delta(\omega_{\mathbf{k}\beta}+\omega_{\mathbf{k}'\beta'}-\omega_p) \times h(L\Delta_{\mathbf{k}\mathbf{k}'})h_{\mathrm{tr}}(\boldsymbol{\kappa},\boldsymbol{\kappa}',\boldsymbol{\kappa}_p), \quad (18)$$

where

$$h(x)=\frac{1-e^{-ix}}{ix}, \quad (19)$$

$$h_{tr}(\boldsymbol{\kappa},\boldsymbol{\kappa}',\boldsymbol{\kappa}_p)=\frac{1}{A}\int_A d^2\rho e^{i(\boldsymbol{\kappa}_p-\boldsymbol{\kappa}-\boldsymbol{\kappa}')\cdot\boldsymbol{\rho}}, \quad (20)$$

$$\Delta_{\mathbf{k}\mathbf{k}'}=k_{pz}-k_z-k_z', \quad (21)$$

and

$$\Gamma=\frac{-i}{\hbar}E_{\boldsymbol{\omega}\beta}E_{\boldsymbol{\omega}'\beta'}2\pi\epsilon_0\chi_{\beta\beta' p}E_0AL. \quad (22)$$

Γ is called the parametric gain index. It is proportional to the second order electric susceptibility χ_{abc}. In (22), $E_{\omega\beta}=e_\omega/n_\beta(\omega)$, and E_0 is the amplitude of the pump beam. A is the cross sectional area of the crystal illuminated by the pump and L is the length of the crystal. In Eq. (21), the z components of the wave numbers are evaluated inside the crystal and are given by Eq. (14). The δ function in (18) comes from the steady-state assumption. The function h comes from the integral over the length of the crystal. In computing the integral over the transverse coordinates in the crystal, (20), the pump beam is assumed to be a monochromatic plane wave traveling in the $\boldsymbol{\kappa}_p+k_{pz}\hat{\boldsymbol{e}}_z$ direction.

In the limit of a crystal with infinite length and cross section, illuminated by a pump beam of infinite cross section, h and h_{tr} become δ functions which lead to the wave-number phase matching condition. When combined with the steady-state assumption, these give the conditions of perfect phase matching:

$$\mathbf{k}_p=\mathbf{k}+\mathbf{k}', \quad (23)$$

$$\omega_p=\omega_{\mathbf{k}\beta}+\omega_{\mathbf{k}'\beta}. \quad (24)$$

If the pump incident on the face of the crystal is of the form

$$E_p=E_0f(\boldsymbol{\rho})e^{-i\omega_p t}, \quad (25)$$

and if it propagates with negligible diffraction, then h_{tr} must be multiplied by the Fourier transform of $f(\boldsymbol{\rho})$, $F(\boldsymbol{\kappa}_p)$:

$$h_{tr}(\boldsymbol{\kappa},\boldsymbol{\kappa}',\boldsymbol{\kappa}_p)\mapsto\int d\boldsymbol{\kappa}_p F(\boldsymbol{\kappa}_p)h_{tr}(\boldsymbol{\kappa},\boldsymbol{\kappa}',\boldsymbol{\kappa}_p). \quad (26)$$

Γ is slowly varying over the spectral range of the beams. It determines the detailed field distribution over the down-converted beams but plays a secondary role to the phase matching. In the calculations below it will be taken to be constant over the range of the down-converted beams detected.

A. Type-II phase matching

In this section we consider phase matching and discuss the shape of the down-converted beam. The pump beam will be assumed to be a monochromatic plane wave traveling along the z axis. Furthermore, it will be assumed that the area of the crystal illuminated by the pump is large enough so that h_{tr} becomes a δ function. This latter condition requires that if the beam illuminates an area of radius a, then

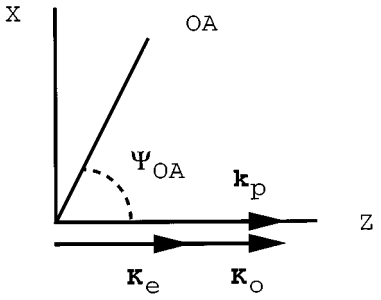

FIG. 2. Collinear perfect phase matching: OA, optic axis of the crystal, lies in the x-z plane.

$\kappa a \gg 1$. Since a is of the order of millimeters and κ is of the order of inverse micrometers in most experiments, this condition is satisfied.

We begin with type-II phase matching. Although the phase matching equations can be solved numerically, it is edifying to look at approximate solutions which lead to a clearer picture of the physics. The approximation is based on two facts. First, most experiments are carried out for small angles, so that we may take $|\boldsymbol{\kappa}| \ll \omega/c$. Second, the range of frequencies reaching each detector, $\Delta\omega$, is limited so that $\Delta\omega \ll \omega$.

Assume that the crystal has been cut so that for collinear down-conversion perfect phase matching holds (Fig. 2):

$$\Omega_e + \Omega_o = \omega_p, \quad (K_e + K_o)\hat{\mathbf{e}}_z = k_p \hat{\mathbf{e}}_z, \tag{27}$$

where

$$K_e = \frac{n_e(\Omega_e, \Psi_{\mathrm{OA}})\Omega_e}{c}, \quad K_o = \frac{n_o(\Omega_o)\Omega_o}{c}, \tag{28}$$

and Ψ_{OA} is the angle between the z axis and the optic axis which we take to lie in the x-z plane. Recall that

$$\frac{1}{n_e(\Omega_e, \Psi_{\mathrm{OA}})^2} = \frac{\cos^2\Psi_{\mathrm{OA}}}{n_o(\Omega_e)^2} + \frac{\sin^2\Psi_{\mathrm{OA}}}{n_e(\Omega_e)^2}, \tag{29}$$

where $n_o(\Omega_e)$ and $n_e(\Omega_e)$ are the principal indices of refraction evaluated at the e-ray frequency [16]. Throughout this paper we shall denote the collinear perfect phase matched frequencies and wave numbers by capital letters as in (27) and (28).

Next consider the noncollinear case (Fig. 3). From the steady state, and the broad beam conditions, we have

$$\omega_e + \omega_o = \omega_p, \tag{30}$$

$$\boldsymbol{\kappa}_e + \boldsymbol{\kappa}_o = \mathbf{0}. \tag{31}$$

To compute Δ, defined in Eq. (21), let

$$\omega_r = \Omega_r + \nu_r, \tag{32}$$

for $r = o$ and e, where $|\nu_r| \ll \Omega_r$. Expanding to first order in κ^2 and ν we get

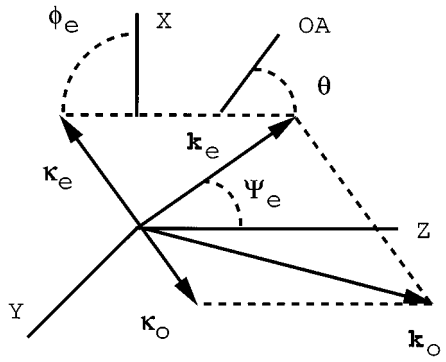

FIG. 3. The e ray and the o ray lie in a plane making an angle ϕ_e with respect to the x-z plane. The $\boldsymbol{\kappa}_a$ are the transverse components of the wave vectors, and θ is the angle between $\mathbf{k}_e$ and the optic axis of the crystal.

$$k_{oz} = \sqrt{k_o^2 - \kappa_o^2} = k_o - \frac{\kappa_o^2}{2K_o}, \tag{33}$$

and

$$k_o = \frac{n_o(\omega_o)}{c} = K_o + \frac{\nu_o}{u_o}. \tag{34}$$

In the second term of (33), we replaced k_o by K_o since the difference is higher than first order. For the same reason the group velocity of the o ray, u_o, is evaluated at Ω_o in (34). The expansion for k_{ez} is complicated by its dependence on the angle between $\mathbf{k}_e$ and the optic axis. In Appendix B we show that

$$k_{ez} = K_e + \frac{\nu_e}{u_e} - \kappa_{ex}N - \frac{\kappa_e^2}{2K_e}, \tag{35}$$

where u_e is the group velocity for the e ray evaluated at Ω_e and Ψ_{OA}, and

$$N = \frac{\partial \ln[n_e(\Omega_e, \Psi_{\mathrm{OA}})]}{\partial \Psi_{\mathrm{OA}}}. \tag{36}$$

It follows from (27) and (30) that $\nu_o = -\nu_e \equiv -\nu$, and

$$\Delta = \nu D - \frac{N^2\overline{K}}{4} + \frac{1}{\overline{K}}\left(\boldsymbol{\kappa}_e + \frac{N\overline{K}}{2}\hat{\boldsymbol{e}}_x\right)^2, \tag{37}$$

where

$$\frac{1}{\overline{K}} = \frac{1}{2}\left(\frac{1}{K_o} + \frac{1}{K_e}\right), \tag{38}$$

$$D = \frac{1}{u_o} - \frac{1}{u_e}. \tag{39}$$

For perfect phase matching $\Delta = 0$. In this case, for fixed ν, (37) is the equation for a circle in the κ plane. The circle

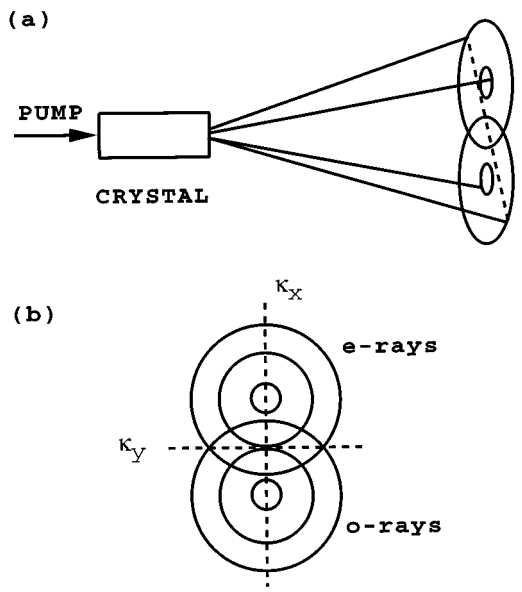

FIG. 4. Two sets of conjugate rings are shown for type-II down-conversion for N negative. In (a) a pair of conjugate points are joined by a dashed line. In (b) some circles of constant ω are illustrated. The circles corresponding to $\omega_e=\omega_o$ are tangent to the κ_y axis.

is centered at $-(NK/2)\hat{\boldsymbol{e}}_x$ and has a radius equal to $\sqrt{N^2K^2/4-\nu DK}$. When $\nu=0$ the circle touches the origin in the $\boldsymbol{\kappa}$ plane and is tangent to the κ_y axis (Fig. 4). The o rays make a complementary circle at $-\boldsymbol{\kappa}_e$. If $D>0$, the circles shrink as ω_e increases and ω_o decreases. The circles vanish when the square root vanishes. For ν negative and decreasing, the radii of the circles increase and the e-ray and o-ray circles overlap [22]. A pair of conjugate circles intersect at points on the κ_y axis with $\kappa=\sqrt{-\nu|D|K}$. The center of each set of circles lies in the plane of the optic axis and the pump wave vector. The e ray lies in the positive κ_x half plane for negative N ($n_e<n_o$).

In order to understand why the circles are offset, let us consider the circle associated with collinear perfect phase matching, Eq. (27). The vectors $\mathbf{k}_o$ with angular frequency Ω_o form a sphere in wave-number space. Therefore as $\boldsymbol{\kappa}_o$ increases, k_{oz} decreases. To satisfy Eq. (23), k_{ez} and therefore $k_e(\Omega_e,\theta)$ must increase, where θ is the angle between $\mathbf{k}_e$ and the optic axis, Fig. 3. For a negative birefringent crystal, $n_e(\omega)<n_o(\omega)$, this requires that θ decreases, which in our case means that $\boldsymbol{\kappa}_e$ lies in the upper half $\boldsymbol{\kappa}$ plane.

The offset is determined by N, which is given by

$$N=\frac{1}{2}n_e^2(\Omega_e,\Psi_{\mathrm{OA}})\left(\frac{1}{n_o^2(\Omega_e)}-\frac{1}{n_e^2(\Omega_e)}\right)\sin(2\Psi_{\mathrm{OA}}). \tag{40}$$

The dominant term in fixing the center of the circle is $\sin(2\Psi_{\mathrm{OA}})$, which vanishes for $\Psi_{\mathrm{OA}}=0$ or 90°. The former case corresponds to type-I down-conversion in which both beams are o rays, and the latter case is sometimes referred to as noncritical phase matching.

Outside the crystal the angle between the wave vector and the z axis, θ_r, is given by $\sin\theta_r=c\kappa_r/\omega_r$ for $r=o$ or e. This means that outside the crystal the conjugate circles have different radii when $\omega_e\neq\omega_o$.

To get a quantitative idea of the nature of perfect phase matching, consider some typical numbers for a beta barium borate (BBO) crystal cut so $\Psi_{\mathrm{OA}}=49°$ and pumped at 350 nm. Then $K=14.6\ \mu\mathrm{m}^{-1}$, $N=-0.07$, and $cD=0.07$. For the degenerate case, the wavelength outside the crystal is 0.7 μm, and the center of the circle is a distance of 0.52 $\mu\mathrm{m}^{-1}$ from the origin of the $\boldsymbol{\kappa}$ plane. The rays for this circle form a cone with an opening angle of 0.12 rad viewed from outside the crystal. Suppose it were possible to see the perfect phase matching. Then each point on a given e-ray circle would correspond to a unique frequency and wave number. If we were to look at the perfect phase matching through a filter centered at 0.7 μm with a width of 1.0 nm, we would see a band of down-converted radiation of thickness $\Delta\kappa=0.13\ \mu\mathrm{m}^{-1}$ corresponding to an angular spread of about 14 mrad. For this crystal and pump, the wavelengths at which the circles vanish are given by $\lambda_e=0.68$ μm and $\lambda_0=0.72$ μm.

Inside a uniaxial crystal the Poynting wave vector for an e ray is not parallel to the wave vector except at $\Psi_{\mathrm{OA}}=90°$. The Poynting vector lies in the plane of the optic axis and the wave vector making an angle δ with the wave vector where $\tan\delta=-N$. δ is defined as positive if the Poynting vector lies between the optic axis and the wave vector. The polarization vectors are usually associated with electric field vectors which are orthogonal to the Poynting vector. The e polarization is in the plane of the optic axis and the wave vector, and the o polarization is perpendicular to that plane; consequently, the directions of the polarization vectors change as a given pair of circles is traversed.

To observe the rings, experimentalists take pictures through narrow filters with the detectors close to the surface of the crystal. The resulting picture is related to the single-photon counting rate. For the case discussed above, it is not difficult to compute this counting rate. It is convenient to define the transverse wave number from the center of the circle, $\boldsymbol{p}=\boldsymbol{\kappa}_e+(NK/2)\hat{\boldsymbol{e}}_x$. If the filter has a Gaussian shape centered at the frequency of the ring, $\Omega_e+\overline{\nu}$, then the counting rate into a small region of the $\boldsymbol{\kappa}$ plane, d^2p, is

$$R_1=Cd^2p\int_{-\infty}^{\infty}d\nu e^{-\gamma^2(\nu-\overline{\nu})^2}\times\mathrm{sinc}^2\left(\left[(\nu-\overline{\nu})D+(\overline{p^2}-p^2)\frac{1}{\overline{K}}\right]\frac{L}{2}\right), \tag{41}$$

where C is approximately constant and $\overline{p}=\frac{1}{2}|N|\overline{K}$. The effect of the breakdown of perfect phase matching due to the finite length of the crystal gives rise to the sinc-squared function, (19). Taking the full width of the sinc function to be 2π, we see that the natural spectral linewidth of a ring is given by

$$\delta\lambda=\frac{2\lambda_e^2}{c|D|L}, \tag{42}$$

where $\lambda_e = 2\pi c/\Omega_e$. If the filter bandwidth is large, $\Delta\lambda \gg \delta\lambda$, then R_1 is constant. For a narrow bandwidth filter, $\Delta\lambda \ll \delta\lambda$, the Gaussian in (41) can be replaced by a δ function and the natural width of the circle will be given by

$$\delta\kappa = \frac{2\pi\overline{K}}{L\overline{p}} = \frac{4\pi}{L|N|}. \tag{43}$$

The natural width of the circle and the natural spectral linewidth both scale as $1/L$.

We give some typical numbers for the example discussed above. For a 1 mm crystal, a point detector that would detect a single frequency for perfect phase matching actually detects a spectral bandwidth (42) of about 14 nm. This corresponds to a coherence length of about 37 μm for a single photon. If the bandwidth of the filter is smaller than this, the filter determines the coherence length of the photon. The light radiated from the circle will be quasimonochromatic for experiments that use small pinholes to pick out a part of the down-converted radiation and involves transverse dimensions of a few μm [25]. For a narrow bandwidth filter, the band of radiation in the κ plane determined by Eq. (43) has a full width of about 0.18 $\mu\mathrm{m}^{-1}$. This corresponds to an angular spread of about 20 mrad outside the crystal. These results are borne out by exact calculations.

The natural spectral linewidth can be understood by noting that the pump excites nonlinear dipole oscillations which radiate at the signal and idler frequencies. For perfect phase matching all the dipoles in the crystal are in phase. However, the beams generated at the input face of the crystal reach the output faces of the crystal with a relative phase shift of $|D|L|\omega_e - \omega_o|$. Because of this, beams radiated with frequencies inside the natural spectral bandwidth will radiate coherently with these beams if this phase shift is less than $\pi/2$.

The natural width of the circles can be understood in a similar manner by noting that rays generated at the input face of the crystal with $\boldsymbol{\kappa} \neq \underline{0}$ arrive at the output face with a relative phase of $-(\kappa^2/\overline{K})L$. Therefore, if an e ray is generated with $\boldsymbol{\kappa} + \delta\boldsymbol{\kappa}$, the e ray and its conjugate o ray will radiate coherently with the original beam if $\boldsymbol{\kappa} + \delta\boldsymbol{\kappa}$ lies within the natural width of the circle.

B. Type-I phase matching

For completeness we discuss type-I phase matching for the case that the pump is an e ray and the signal and idler are both o rays. We shall see that in the nondegenerate case ($\Omega_s \neq \Omega_i$), the results are similar to the type-II case because D does not vanish. In the degenerate case $D = 0$, and we must go to higher order in the frequency, ν defined in Eq. (32), when calculating Δ. The case of an o-ray pump with the signal and idler e rays is similar but it is necessary to account for group velocity dependence on the angle between the propagation direction and the optic axis as in type II.

If the crystal is cut so that there is nondegenerate collinear phase matching ($\Omega_s \neq \Omega_i$), a calculation similar to the one above leads to the equation

$$\Delta = -\nu D + \frac{\kappa_s^2}{\overline{K}}, \tag{44}$$

where

$$\omega_s = \Omega_s + \nu, \tag{45}$$

$$\frac{1}{\overline{K}} = \frac{1}{2}\left(\frac{1}{K_s} + \frac{1}{K_i}\right), \tag{46}$$

$$D = \frac{1}{u_o(\Omega_s)} - \frac{1}{u_o(\Omega_i)}. \tag{47}$$

For perfect phase matching this leads to circles centered around the origin of the κ plane. Let $\Omega_s > \Omega_i$ so that, generally, $n_o(\Omega_s) > n_o(\Omega_i)$ and $D > 0$, then the radius of the circle increases from 0 as the signal frequency increases and the idler frequency decreases. In viewing or photographing these circles, the image of the idler circle is at a larger angle than that of the signal. Of course, what is seen depends on the details of frequency response of the detector.

The frequency bandwidth of a given circle is determined by Eq. (42) with λ_e replaced by λ_s or λ_i. The width of a circle of given frequency is given by the first expression in Eq. (43), where $\overline{p}$ is the radius of the circle in κ space.

If the crystal is cut so that the collinear phase matching is degenerate ($\Omega_s = \Omega_i$) then D will vanish and the expansion of Δ must be carried to second order in the signal frequency.

$$\Delta = -\nu^2 D' + \frac{\kappa_s^2}{K_o}, \tag{48}$$

where

$$k_p = 2K_o, \quad \omega_p = 2\Omega_0, \quad D' = \frac{d}{d\Omega_o}\frac{1}{u_o(\Omega_o)}.$$

D' is generally positive. The natural spectral bandwidth of a circle is

$$\delta\lambda = \lambda_o^2\sqrt{\frac{1}{2\pi c^2 D' L}}, \tag{49}$$

where $\lambda_o = 2\pi c/\Omega_o$, and the thickness of a circle is

$$\delta\kappa = \sqrt{\frac{4\pi K_o}{L}}. \tag{50}$$

Both $\delta\lambda$ and $\delta\kappa$ scale as $1/\sqrt{L}$. To get a quantitative feel for these quantities we consider a potassium dihydrogen phosphate (KDP) crystal cut so $\Psi_{\mathrm{OA}} = 47°$ with a pump at 0.35 μm. Then $K_0 = 12.6$ $\mu\mathrm{m}^{-1}$ and $c^2 D' = 3.4\times10^{-3}$ μm, so that $\delta\lambda = 0.15$ μm and $\delta\kappa = 1.0$ $\mu\mathrm{m}^{-1}$ for a 1 mm crystal.

There are cases in which it is not possible to satisfy perfect phase matching for the collinear case. We leave this case as an exercise.

IV. TWO-PHOTON OPTICS

In the cases discussed below, it is assumed that the pump is a monochromatic plane wave traveling along the z axis

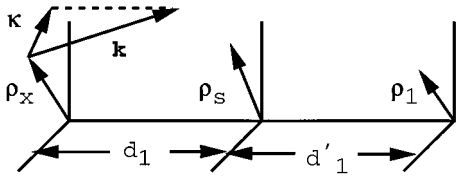

FIG. 5. The output face of the crystal forms the X plane, the optical system is specified by a aperture function in the S plane, and detector 1 is located at $\boldsymbol{\rho}_1$ in a plane at the distance z_1 from the crystal. The vector $\boldsymbol{\kappa}$ is the transverse component of the wave vector $\mathbf{k}$ of magnitude ω/c.

with cross section large enough so that h_{tr} can be taken to be a δ function:

$$h_{tr}(\boldsymbol{\kappa},\boldsymbol{\kappa}',\mathbf{0})=\delta_{\boldsymbol{\kappa}+\boldsymbol{\kappa}'\mathbf{0}}. \tag{51}$$

We will assume that the range of frequencies detected is limited so that we may take

$$\omega_r=\Omega_r+\nu_r, \tag{52}$$

where $|\nu_r|\ll\Omega_r$ and Ω_r is constant. We will confine our discussion to type-II down-conversion. For signal and idler pairs, we will always take $\Omega_s+\Omega_i=\omega_p$.

A. Singles counting rate

First consider the singles counting rate for an experiment of the type shown in Fig. 1(a). It is not difficult to see using (17) and (18) with (51) that

$$\langle 0|a_{\mathbf{k}_e}E_1^+|\Psi\rangle=\Gamma' e_{\omega_o}e^{-i\omega_o t_1}g_1(-\boldsymbol{\kappa}_e,\omega_o,\boldsymbol{\rho}_1,z_1)h(\Delta L). \tag{53}$$

All the slowly varying constants have been absorbed into Γ', $\mathbf{k}_e=\boldsymbol{\kappa}_e+\sqrt{(\omega_e/c)^2-\kappa_e^2}\hat{\mathbf{e}}_z$, $\omega_o=\omega_p-\omega_e$, and Δ is given by (37). The location of point detector one is at $\boldsymbol{\rho}_1+z_1\hat{\mathbf{e}}_z$, t_1 is the detection time, and we have assumed that the detector does not have a polarization analyzer in front of it. The singles counting rate is independent of time and may be written using Eq. (84) as

$$R_1=R_0\sum_{\mathbf{k}_e}\left|S_1\left(-\boldsymbol{\kappa}_e-\frac{\omega_o}{c}P_1'\boldsymbol{\rho}_1,\frac{\omega_o}{c}P_1'\right)\right|^2|h(\Delta L)|^2, \tag{54}$$

where S_1 is the Fourier transform of the aperture function modeling the optical system in front of detector 1 and is defined in (85), and $P_1'=1/d_1'$, Fig. 5. The frequency dependence of S_1 occurs in two places. The dependence on frequency in the second argument can be removed by using a lens and judicious choice of the detector plane, as discussed in Appendix A. The frequency dependence in the first argument can be neglected in the paraxial approximation. For these reasons, we replace ω_o in S_1 with Ω_o. To evaluate the sum, we convert it into an integral in the usual way, and then change variables to the beam invariants:

$$\sum_{\mathbf{k}_e}\rightarrow\frac{V}{(2\pi)^3}\int d^3k_e\rightarrow\frac{V}{(2\pi)^3}\int d^2\kappa_e d\omega_e\frac{\omega_e}{c^2k_z}. \tag{55}$$

Using (52), the counting rate becomes

$$R_1=R_0\int d^2\kappa_e\left|S_1\left(-\boldsymbol{\kappa}_e-\frac{\Omega_o}{c}P_1'\boldsymbol{\rho}_1,\frac{\Omega_o}{c}P_1'\right)\right|^2\times\int d\nu|\mathrm{sinc}(\Delta L/2)|^2. \tag{56}$$

All the slowly varying quantities have been absorbed into R_0.

The integral over ν will be determined by the form of filtering used. Recall that for a point detector and perfect phase matching there would be a unique frequency incident on the detector from each direction. The breakdown of perfect phase matching, determined by the sinc function, allows a range of frequencies to impinge on the detector from each direction. In experiments, the filtering may be done directly by placing a filter in the beam or indirectly by using a small pinhole to limit the range of $\boldsymbol{\kappa}$ that enter the detector. We have seen that this also limits the frequencies that reach the detector. If the bandwidth of the frequency filter is large compared to the natural spectral width of the biphoton, (42), the integral over the frequency will give a constant and the integral over the transverse components of the wave number will also give a constant for all $\boldsymbol{\rho}_1$ in the paraxial region.

For a filter with center frequency $\Omega_e+\overline{\nu}$ and with a width small compared to the natural spectral width of the biphoton, we can set the $\nu=\overline{\nu}$ in the sinc function. The sinc function will be nonvanishing in a disk in $\boldsymbol{\kappa}$ space as discussed in Sec. III. In general, the width of the disk is large enough to wash out any details on scales larger than tens of micrometers. To see this suppose that we take our optical system to be a lens of focal length f with aperture radius a. Then if the detector is placed in the focal plane of the lens, $P_1'=1/f$, S becomes the Fourier transform of the aperture (A9). The counting rate becomes

$$R_1=R_0\int d^2\kappa\left(\frac{J_1(\kappa a)}{\kappa a}\right)^2\mathrm{sinc}^2(\Delta' L/2), \tag{57}$$

where $J_1(z)$ is a Bessel function and

$$\Delta'=\overline{\nu D}-\frac{N^2\overline{K}}{4}+\left(\boldsymbol{\kappa}-\frac{\Omega_o}{cf}\boldsymbol{\rho}_1+\frac{N\overline{K}}{2}\hat{\mathbf{e}}_x\right)^2\frac{1}{\overline{K}}. \tag{58}$$

If the aperture is of the order of tenths of millimeters, then the range of the κ integral is determined by the Bessel function to be a few mm^{-1}. Over this range the sinc function is approximately constant for ρ_1/f less than 10 mrad. This means that the diffraction effects of the slit cannot be seen. Furthermore, if the single aperture is replaced by a pair of apertures, the Young's interference fringes will be washed out [11]. Note that the form of (57) is consistent with the advanced wave picture in which the e ray is visualized as being emitted by an incoherent broadband source with an area of the order of $\mu\mathrm{m}^2$.

B. Coincidence counting rate

We now consider the coincident counting rate for the experiment shown in Fig. 1(a). As in the example above, we only place an optical system in beam 1. The coincident

counting rate is given by Eq. (16). Using the results of Appendix A, the two-photon amplitude is

$$A_{12}=A\sum_{\mathbf{k}_1,\mathbf{k}_2} e^{-i(\omega_1 T_1+\omega_2 T_2)}\psi\left(\rho_1,\frac{\omega_1}{c}P_1'\right)\times S_1\left(\boldsymbol{\kappa}_1-\omega_1 P_1'\boldsymbol{\rho}_1,\frac{\omega_1}{c}P_1'\right)\times\psi\left(\kappa_1,-\frac{c}{\omega_1 P_1}\right)\psi\left(\kappa_2,-\frac{c}{\omega_2 P_2}\right)e^{i\boldsymbol{\kappa}_2\cdot\boldsymbol{\rho}_2}\times\delta(\omega_1+\omega_2-\omega_p)\,\delta_{\boldsymbol{\kappa}_1+\boldsymbol{\kappa}_2,\mathbf{0}}\,h(L\Delta), \tag{59}$$

where $T_r=t_r-z_r/c$ for $r=1$ and 2. We denote T_1-T_2 by T_{12}, and convert the sums to integrals. All the slowly varying terms and overall phase factors are absorbed into A. We introduce the beam invariants and use (52). In (59) the ν dependence in ψ and S_1 can be dropped in the paraxial approximation. Then we can write

$$A_{12}=A\int d^2\kappa\,\psi\left(\kappa,-\frac{c}{\Omega_1 P_1}\right)\psi\left(\kappa,-\frac{c}{\Omega_2 P_2}\right)\times e_2^{-i\boldsymbol{\kappa}\cdot\boldsymbol{\rho}}S_1\left(\boldsymbol{\kappa}-\omega_1 P_1'\boldsymbol{\rho}_1,\frac{\omega_1}{c}P_1'\right)\times\int d\nu e^{-i\nu T_{12}}h(L\Delta). \tag{60}$$

The integral over ν can be evaluated using

$$h(L\Delta)=\mathrm{sinc}(\nu-\nu_0)\frac{LD}{2},$$

$$\nu_0=\frac{1}{D}\left[\frac{N^2\overline{K}}{4}-\left(\boldsymbol{\kappa}-\frac{N\overline{K}}{2}\hat{\boldsymbol{e}}_x\right)^2\frac{1}{\overline{K}}\right]. \tag{61}$$

For a broadband filter, the integral is simply the Fourier transform of a sinc function, which leads to a rectangular function [4]:

$$\int d\nu e^{-i\nu T_{12}}h(L\Delta)=\frac{2\pi}{DL}e^{-i\nu_0 T_{12}}\Pi(T_{12},-DL), \tag{62}$$

where $\Pi(x,a)$ is one if $x\in(0,a)$ and vanishes otherwise. For a narrower filter, the Π function will be smoothed and broadened. This will not change the results significantly.

Next, we do the κ integration using Eq. (A9) and the fact that the integrand reduces to a Gaussian. Again, absorbing constants and overall phase factors into A, we find

$$A_{12}=A\Pi(T_{12},-DL)\int d^2\rho_s s_1(\boldsymbol{\rho}_1)\times e^{-i\boldsymbol{\rho}_s\cdot\boldsymbol{\kappa}_0(T_{12})}\psi(\rho_s,\Sigma(T_{12})), \tag{63}$$

$$\boldsymbol{\kappa}_0(T_{12})=\left(\boldsymbol{\rho}_2+\frac{NT_{12}}{D}\hat{\boldsymbol{e}}_x\right)\Sigma(T_{12})+\boldsymbol{\rho}_1\frac{\Omega_1}{c}P_1', \tag{64}$$

$$\frac{1}{\Sigma}=\frac{c}{\Omega_1}d_1+\frac{c}{\Omega_2}z_2, \tag{65}$$

$$\frac{1}{\Sigma(T_{12})}=\frac{1}{\Sigma}+\frac{2T_{12}}{\overline{KD}}. \tag{66}$$

The interpretation of A_{12} is now clear. The integral is a Fourier transform evaluated at $\boldsymbol{\kappa}_0(T_{12})$ of the aperture function, s_1, weighted by a Fresnel factor. In standard optics it is well known that the Fresnel factor can be removed by placing a converging lens of focal length f in the aperture plane and placing the detectors in the appropriate optical planes (Ref. [21]). Because of the T_{12} dependence, it is not evident that we can do this. Note that this formula shows that, in general, spatial and temporal effects cannot be separated in discussing the two-photon transverse correlation.

Let us examine the terms containing T_{12}. First, we have

$$\Sigma(T_{12})=\frac{1}{1+\alpha(T_{12})}\Sigma, \tag{67}$$

$$\alpha(T_{12})=\Sigma\frac{2L}{\overline{K}}\left(\frac{T_{12}}{LD}\right). \tag{68}$$

The magnitude of T_{12}/LD lies between 0 and 1. The combined first two factors in (68) are of the order of the ratio of the crystal length to the detector distance, $2L/(nz)$, where n is some average index of refraction of the crystal. It comes from the uncertainty in the optical path between the source of the pair of photons and the detectors. This factor is usually small compared to one, typically, it is of the order of 10^{-3}. Therefore we may drop $\alpha(T_{12})$ and take $\Sigma(T_{12})\approx\Sigma$.

Next,

$$\boldsymbol{\kappa}_0(T_{12})=\boldsymbol{\kappa}_0(0)+\delta\boldsymbol{\kappa}_0(T_{12}),$$

$$\delta\boldsymbol{\kappa}_0(T_{12})=\Sigma NL\left(\frac{T_{12}}{DL}\right)\hat{\boldsymbol{e}}_x+\boldsymbol{\rho}_2\Sigma\,\alpha(T_{12}), \tag{69}$$

where only the leading terms in T_{12} have been retained. In the first term in $\delta\boldsymbol{\kappa}_0(T_{12})$, NL is the walk-off distance of an e ray across the crystal. Σ is of the order of a free space wave vector times the distance to the detector. If we imagine holding the location of detector 1 fixed, this term represents an uncertainty in the optimal position of detector 2 ($\boldsymbol{\kappa}_0=\mathbf{0}$) due to the finite extent of the biphoton. That is, for pairs created closer to the input face of the crystal, the optimal $\boldsymbol{\rho}_2$ decreases if $N<0$. When this term is multiplied by a typical transverse dimension, of the order of millimeters, it will be much smaller than one. The second term in $\delta\boldsymbol{\kappa}_0(T_{12})$ is even smaller.

We can now drop the T_{12} dependence in $\Sigma(T_{12})$ and $\delta\boldsymbol{\kappa}_0(T_{12})$. This means that as a practical matter in typical experiments the width, DL, of the biphoton does not effect the transverse correlations. Set $P_1'+(c/\Omega_1)\Sigma=1/f$, so that A_{12} is proportional to the Fourier transform of $t(\boldsymbol{\rho})$, defined in (A11). That is, we choose

$$\frac{1}{d_1'}+\frac{1}{d_1+(\Omega_1/\Omega_2)z_2}=\frac{1}{f}. \tag{70}$$

Note that $(c/\Omega_1)(1/\Sigma)=d_1+(\Omega_1/\Omega_2)z_2$ is the distance from the screen to the crystal plus the distance from the crystal to detector 2 weighted by the ratio of the free space wavelengths.

For fixed $\boldsymbol{\rho}_1$ the Fourier transform of $t(\boldsymbol{\rho})$ will be traced out as $\boldsymbol{\rho}_2$ is varied. The magnification of the inverted image can be found by setting $T_{12}=0$ in (64), it is given by $f/(d_1'-f)$. Finally, using (A12)

$$R_2=R_0\left|S_1\left(\boldsymbol{\kappa}_0(0),\frac{\Omega_1}{c}\frac{1}{f}\right)\right|^2. \tag{71}$$

Equation (70) is of the form of the equation relating the object and image plane to the focal length of a lens in geometrical optics. The appearance of this equation is what leads us to refer to the imaging effects as two-photon geometrical optics. The general form of (71) shows that we can expect to see all the usual types of diffractive and interferometric phenomena discussed in physical optics. It is important to note that the image in (71) appears in the coincidence counting and is not localized at either detector.

V. TWO-PHOTON COHERENCE

There are several types of coherence factors which enter into the discussion of the biphoton which have been discussed in the literature [15]. For example, the coherence length of single photons plays an important role in the discussion of two-photon interference experiments [27,28]. We wish to suggest a definition of the two-photon transverse coherence.

Consider the case of the idealized experiment of the preceding section using two point detectors. We consider a lens placed at the output face of the crystal so that $d_1=0$ and $d_1'=z_1$. Take $z_1=f$, which is equivalent to detector 1 being fixed at a point $\boldsymbol{\rho}_1$ in the far field region. Choose $\boldsymbol{\kappa}_0(0)=0$, so that $\boldsymbol{\rho}_2=-(\lambda_1 z_2/\lambda_2 z_1)\boldsymbol{\rho}_1$. The λ's are the free space wavelengths of the detected radiation. Holding $\boldsymbol{\rho}_2$ fixed and letting $\boldsymbol{\rho}_1$ vary, it is easy to show that Eq. (64) becomes

$$\boldsymbol{\kappa}_0(T_{12})=\delta\boldsymbol{\rho}_1\frac{\Omega_1}{cz_1}+\Sigma(T_{12})[NL\hat{\boldsymbol{e}}_x+\alpha(T_{12})\boldsymbol{\rho}_2], \tag{72}$$

where $\delta\boldsymbol{\rho}_1$ is the variation of $\boldsymbol{\rho}_1$. Furthermore, take

$$s_1(\boldsymbol{\rho}_s)=\psi(\rho_s,-F)e^{-\rho_s^2/2a^2}. \tag{73}$$

This is an approximate way to represent the pump beam cross section by a Gaussian. Then,

$$R_2=R_0\exp\left[-\frac{a^2}{1+[\Sigma(T_{12})a^2\alpha(T_{12})]^2}\times\left(\delta\boldsymbol{\rho}_1\frac{\Omega_1}{cz_1}+\Sigma(T_{12})\{NL\hat{\boldsymbol{e}}_x+\alpha(T_{12})\boldsymbol{\rho}_2\}\right)\right]. \tag{74}$$

Since $\Sigma(T_{12})a^2\alpha(T_{12})\ll 1$, the spot size corresponding to the point detector 2 is defined by setting $T_{12}=|D|L$ so that

$$\frac{|\delta\boldsymbol{\rho}_1|}{z_1}=\frac{\lambda_1}{2\pi}\left(\frac{1}{a}+\Sigma(L|D|)\left|NL\hat{\boldsymbol{e}}_x+\alpha(L|D|)\boldsymbol{\rho}_2\right|\right). \tag{75}$$

The first term is just the diffraction from the Gaussian aperture, the second term is the effect of the biphoton. It is this term that we propose to define as the angular transverse coherence of the biphoton. Let us rewrite this in a form that makes it clearer. Since $d_1=0$, $\Sigma=\Omega_2/cz_2$, and $\alpha(|D|L)=2\Omega_2/cKz_2$, and

$$\frac{|\delta\boldsymbol{\rho}_1|}{z_1}=\frac{\lambda_1}{2\pi a}+\frac{\Omega_2}{\Omega_1}\left|\frac{NL}{z_2}\hat{\boldsymbol{e}}_x+\frac{2\Omega_2}{Kc}\frac{\boldsymbol{\rho}_2}{z_2}\right|, \tag{76}$$

where we have dropped the second term in (66) in writing (76). The two terms in the angular transverse coherence of the biphoton can be identified. One is the ratio of the walk-off in the crystal to the distance to detector 2, NL/z_2. In the second term $n=Kc/2\Omega_2$ is an average index of refraction of the crystal and so the second term is of the order of L/nz_2 times the anglular position of detector two. Although for the experiments reported in the literature, the angular transverse coherence of the biphoton is negligible compared to the first term, it is worthwhile to define this quantity because it is the contribution that comes from the biphoton.

VI. CONCLUSION

We have presented the detailed behavior of the transverse correlation of the two-photon state generated in type-II SPDC. The discussion was limited to point detectors, but it is not difficult to consider detectors of finite size.

We have discussed the emergence of two-photon geometric and physical optics, with emphasis on the importance of the spectral function of the biphoton and the role of classical optics. A detailed discussion of phase matching has allowed us to describe the physics of the beautiful colored rings that can be photographed emerging from the down-conversion crystal [24] and to elucidate the various quantities that play a role in determining them. In particular, the natural spectral bandwidth and the natural width of the rings have been calculated in Eqs. (42) and (43). The transverse correlation leads to interesting spatial filtering effects in the coincident counting rate. These may be studied by examining the correlation functions [14] or by means of physical optics. One result of these studies is to show the intimate relation between the spatial and temporal effects in determining the transverse correlations. Our study of two-photon optics provides a detailed explanation of the reason that the singles counting rates have no structure in experiments such as the ''ghost'' interference experiment [11] but the coincident counting rates show the interference effects. We have suggested a definition of the biphoton transverse coherence which is at present of academic interest because in the experiments reported ordinary diffractive effects are much more important.

ACKNOWLEDGMENTS

I wish to thank my colleagues from the UMBC Quantum Optics Group, Y. H. Shih, A. V. Sergienko, T. B. Pittman, and D. V. Strekalov, for many discussions about the material

in this paper. I also wish to acknowledge instructive discussions with D. N. Klyshko. This work was supported by the Office of Naval Research, Grant No. N00014-91-J-1430.

APPENDIX A: GREEN'S FUNCTIONS

A diffraction limited optical system can be represented in terms of an aperture function. In Fig. 5 the aperture function, defined by $s(\boldsymbol{\rho}_s)$, is located in a plane a distance d_1 from the output face of the crystal and d_1' from the detector. The Green's function introduced in Eq. (15) can be written as

$$g_1(\boldsymbol{\kappa},\omega,\boldsymbol{\rho}_1,z_1)=\int d^2\rho_s\int d^2\rho_x h_\omega(\boldsymbol{\rho}_1-\boldsymbol{\rho}_s,d_1')s_1(\boldsymbol{\rho}_s)\times h_\omega(\boldsymbol{\rho}_s-\boldsymbol{\rho}_x,d_1)e^{i\boldsymbol{\kappa}\cdot\boldsymbol{\rho}_x}, \tag{A1}$$

where $z_1=d_1+d_1'$ and the optical transfer function is defined in the paraxial approximation by [21]

$$h_\omega(\boldsymbol{\rho},d)=\frac{-i\omega}{2\pi c}\frac{e^{i(\omega/c)d}}{d}\psi\left(\rho,\frac{\omega}{cd}\right), \tag{A2}$$

$$\psi\left(\rho,\frac{\omega}{c}P\right)=e^{i(\omega/2c)P\rho^2}. \tag{A3}$$

It is useful to note that [26]

$$\psi^*\left(\rho,\frac{\omega}{c}P\right)=\psi\left(\rho,-\frac{\omega}{c}P\right), \tag{A4}$$

$$\psi\left(\rho,\frac{\omega}{c}(P+P')\right)=\psi\left(\rho,\frac{\omega}{c}P\right)\psi\left(\rho,\frac{\omega}{c}P'\right), \tag{A5}$$

$$\psi\left(|\boldsymbol{\rho}-\boldsymbol{\rho}'|,\frac{\omega}{c}P\right)=\psi\left(\rho,\frac{\omega}{c}P\right)\psi\left(\rho',\frac{\omega}{c}P\right)e^{-i(\omega/c)P\boldsymbol{\rho}\cdot\boldsymbol{\rho}'}, \tag{A6}$$

and the Fourier transform equation

$$\tilde{\psi}(\kappa,P)=\int d^2\rho\,\psi\left(\rho,\frac{\omega}{c}P\right)e^{i\boldsymbol{\kappa}\cdot\boldsymbol{\rho}}=i\frac{2\pi c}{\omega P}\psi\left(\kappa,-\frac{c}{\omega P}\right). \tag{A7}$$

It is now a simple matter to show that

$$g_1(\boldsymbol{\kappa},\omega,\boldsymbol{\rho}_1,z_1)=\frac{-i\omega}{2\pi c}P_1'e^{i(\omega/c)z_1}\psi\left(\rho_1,\frac{\omega}{c}P_1'\right)\times S_1\left(\boldsymbol{\kappa}-\frac{\omega}{c}P_1'\boldsymbol{\rho}_1,\frac{\omega}{c}P_1'\right)\psi\left(\kappa,-\frac{c}{\omega P_1}\right), \tag{A8}$$

$$S_1\left(\boldsymbol{\kappa},\frac{\omega}{c}P_1'\right)=\int d^2\rho_s\psi\left(\rho_s,\frac{\omega}{c}P_1'\right)e^{i\boldsymbol{\kappa}\cdot\boldsymbol{\rho}_s}s_1(\boldsymbol{\rho}_s), \tag{A9}$$

where $P_1=1/d_1$ and $P_1'=1/d_1'$. To interpret (A8), recall that for a plane wave of angular frequency ω, in the paraxial approximation

$$e^{i(k_zd+\boldsymbol{\kappa}\cdot\boldsymbol{\rho})}\approx e^{i(\omega/c)d}\psi\left(\kappa,\frac{c}{\omega}d\right)e^{i\boldsymbol{\kappa}\cdot\boldsymbol{\rho}}, \tag{A10}$$

where $k_z=\sqrt{(\omega/c)^2-\kappa^2}$. Equation (A8) corresponds to the observation of the aperture function illuminated by a plane wave source at the crystal face and observed at the point $\boldsymbol{\rho}_1+z_1\hat{\boldsymbol{e}}_z$.

If we place a converging lens of focal length $1/F$ in the plane of the aperture function, then [21]

$$s_1(\boldsymbol{\rho})=\psi\left(\rho,-\frac{\omega}{c}F\right)t(\boldsymbol{\rho}). \tag{A11}$$

Substituting this into (A9) gives

$$S_1\left(\boldsymbol{\kappa},\frac{\omega}{c}P_1'\right)=\int d^2\rho_s\psi\left(\rho_s,\frac{\omega}{c}(P_1'-F)\right)e^{i\boldsymbol{\kappa}\cdot\boldsymbol{\rho}_s}t(\boldsymbol{\rho}_s), \tag{A12}$$

which becomes the Fourier transform of $t(\boldsymbol{\rho})$ when the detector is in the focal plane of the lens, $P_1'=F$. Note that this result is independent of the frequency of the radiation over the range for which the lens can be assumed to have a constant index of refraction.

APPENDIX B: EVALUATION OF THE SPECTRAL FUNCTION

The evaluation of F has been discussed in [4,13]. We summarize the results here for convenience. For typical experiments the detectors are located a large distance from the crystal and at a small angle with respect to the pump axis so that the paraxial approximation is valid. Therefore Eq. (14) can be expanded

$$k_z=k_\beta(\omega)-\frac{\kappa^2}{2k_\beta(\omega)}+\ldots, \tag{B1}$$

where we drop the higher order terms, and

$$k_\beta(\omega)=\frac{\omega n_\beta(\omega)}{c}. \tag{B2}$$

In most experiments the detectors collect a very narrow band of frequencies, so we may write $\omega_a=\Omega_a+\nu_a$ for $a=o$ and e where $|\nu_a|\ll\Omega_a$ and expand $k_\beta(\omega)$ around Ω_a.

For the o ray,

$$k_o(\omega_o)=K_o+\frac{\nu_o}{u_o}+\ldots, \tag{B3}$$

$$K_o=\frac{\Omega_o n_o(\Omega_O)}{c}, \tag{B4}$$

$$\frac{1}{u_o}=\frac{d}{d\Omega_o}\frac{\Omega_o n(\Omega_O)}{c}, \tag{B5}$$

where u_o is the group velocity of the o ray evaluated at Ω_o. To leading order, we have

$$k_{oz}=K_o+\frac{\nu_o}{u_o}-\frac{\kappa_o^2}{2K_o}. \tag{B6}$$

For type II and nondegenerate type I, we do not have to go to higher order in ν. Referring to Eq. (21) and Eq. (44), we see that ν appears multiplied by the difference between the inverse group velocities of the e ray and o ray.

For the e ray, the index of refraction varies as the direction of the wave number changes. We use the frequency ω_e and $\boldsymbol{\kappa}_e$ as independent variables. Referring to Fig. 3, we have

$$\begin{aligned} k_{ez}&=\sqrt{k_e(\omega_e,\theta)^2-\kappa_e^2}\\ &=K_e+\frac{\nu_e}{u_e}+\frac{\partial k_e}{\partial \boldsymbol{\kappa}_e}\cdot\boldsymbol{\kappa}_e-\frac{\kappa_e^2}{2K_e}, \end{aligned} \tag{B7}$$

where

$$\begin{aligned} \omega_e&=\Omega_e+\nu_e,\\ K_e&=k_e(\Omega_e,\Psi_{\mathrm{OA}}),\\ \frac{1}{u_e}&=\frac{\partial}{\partial\Omega_e}\left(\frac{\Omega_e n_e(\Omega_e,\Psi_{\mathrm{OA}})}{c}\right). \end{aligned} \tag{B8}$$

In expanding k_e it only is necessary to keep the first order term in $\boldsymbol{\kappa}_e$ since the coefficient of this term is small. The coefficient is evaluated at $\omega_e=\Omega_e$ and $\theta=\Psi_{\mathrm{OA}}$. Now we must evaluate the partial derivative of k_e with respect to $\boldsymbol{\kappa}_e$ keeping the frequency fixed. First, we have

$$\frac{\partial k_e}{\partial \boldsymbol{\kappa}_e}=\frac{\omega_e}{c}\frac{\partial n_e(\omega_e,\theta)}{\partial \boldsymbol{\kappa}_e}=\frac{\omega_e}{c}\frac{\partial\theta}{\partial\boldsymbol{\kappa}_e}\frac{\partial n_e(\omega_e,\theta)}{\partial\theta}. \tag{B9}$$

We now consider the projection of k_e on the optic axis:

$$k_e\cos\theta=k_{ez}\cos\Psi_{\mathrm{OA}}+\kappa_{ex}\sin\Psi_{\mathrm{OA}}. \tag{B10}$$

Differentiating with respect to $\boldsymbol{\kappa}_e$ gives

$$\begin{aligned} \frac{\partial k_e}{\partial\boldsymbol{\kappa}_e}\cos\theta-k_e\sin\theta\frac{\partial\theta}{\partial\boldsymbol{\kappa}_e}&=\left(\frac{k_e}{k_{ez}}\frac{\partial k_e}{\partial\boldsymbol{\kappa}_e}-\frac{\boldsymbol{\kappa}_e}{k_z}\right)\cos\Psi_{\mathrm{OA}}\\ &\quad+\frac{\partial\kappa_{ex}}{\partial\boldsymbol{\kappa}_e}\sin\Psi_{\mathrm{OA}}, \end{aligned}$$

$$\delta_{rx}\sin\Psi_{\mathrm{OA}}=k_e\left[N\left(\cos\theta-\frac{k_e}{k_{ez}}\cos\Psi_{\mathrm{OA}}\right)-\sin\theta\right]\frac{\partial\theta}{\partial\kappa_{er}}, \tag{B11}$$

where $r=x$ or y. N is defined in (36) but here it is evaluated at ω_e and θ. Now letting $\omega_e=\Omega_e$, $\theta=\Psi_{\mathrm{OA}}$, and $\boldsymbol{\kappa}_e=\mathbf{0}$, (B11) reduces to

$$\frac{\partial\theta}{\partial\kappa_{er}}=-\delta_{rx}\frac{1}{K_e}. \tag{B12}$$

Substituting this into (B7) gives Eq. (35).

[1] A. A. Malygin, A. N. Penin, and A. V. Sergienko, Dokl. Akad. Nauk SSSR **281**, 308 (1985) [Sov. Phys. Dokl. **30**, 227 (1985)].

[2] D. N. Klyshko, Zh. Éksp. Teor. Fiz. **83**, 1313 (1982) [Sov. Phys. JETP **56**, 753 (1982)].

[3] D. N. Klyshko, Zh. Éksp. Teor. Fiz. **94**, 82 (1988) [Sov. Phys. JETP **67**, 1131 (1988)].

[4] M. H. Rubin, D. N. Klyshko, Y. H. Shih, and A. V. Sergienko, Phys. Rev. A **50**, 5122 (1994).

[5] Y. H. Shih, A. V. Sergienko, M. H. Rubin, T. E. Kiess, and C. O. Alley, Phys. Rev. A **49**, 4243 (1994).

[6] Y. H. Shih, A. V. Sergienko, M. H. Rubin, T. E. Kiess, and C. O. Alley, Phys. Rev. A **50**, 23 (1994).

[7] A. V. Sergienko, Y. H. Shih, and M. H. Rubin, J. Opt. Soc. Am. B **40**, 859 (1995).

[8] T. B. Pittman, Y. H. Shih, A. V. Sergienko, and M. H. Rubin, Phys. Rev. A **51**, 3495 (1995).

[9] X. Y. Zou, L. J. Wang, and L. Mandel, Phys. Rev. Lett. **67**, 318 (1991).

[10] T. P. Grayson and G. A. Barbosa, Phys. Rev. A **49**, 2948 (1994).

[11] D. V. Strekalov, A. V. Sergienko, D. N. Klyshko, and Y. H. Shih, Phys. Rev. Lett **74**, 3600 (1995).

[12] T. B. Pittman, Y. H. Shih, D. V. Strekalov, and A. V. Sergienko, Phys. Rev. A **52**, R3429 (1995).

[13] T. B. Pittman, D. V. Strekalov, D. N. Klyshko, M. H. Rubin, A. V. Sergienko, and Y. H. Shih, Phys. Rev. A **53**, 2804 (1996).

[14] A. Joobeur, B. E. A. Saleh, and M. C. Teich, Phys. Rev. A **50**, 3349 (1994).

[15] D. N. Klyshko, *Photons and Nonlinear Optics* (Gordon and Breach Science Publishers, New York, 1988).

[16] M. Born and E. Wolf, *Principles of Optics*, 6th ed. (Pergamon Press, Oxford, 1980).

[17] D. N. Klyshko, Phys. Lett. A **128**, 1337 (1988).

[18] D. N. Klyshko, Sov. Phys. Usp. **31**, 74 (1988).

[19] Y. Aharonov, D. Albert, A. Casher, and L. Vaidman, Phys. Lett. A **124**, 199 (1987).

[20] W. H. Louisell, A. Yariv, and A. E. Siegman, Phys Rev. **124**, 1646 (1961).

[21] J. W. Goodman, *Introduction to Fourier Optics* (McGraw-Hill Publishing Company, New York, 1968).

[22] It was noted by Shih and Kwiat and, independently, by Garuccio that the radiation from the points of intersection is useful for the study of the Einstein-Rosen-Podolsky paradox when the o ray and e ray have the same frequency [23,24].

[23] A. Garuccio, in *Fundamental Problems in Quantum Theory*, edited by D. Greenberger and A. Zeilinger, Annals of the New York Academy of Sciences Vol. 755 (New York Academy of Sciences, New York, 1995), p. 632.

[24] P. G. Kwiat *et al.*, Phys. Rev. Lett. **75**, 4337 (1995).

[25] Recall the conditions for quasimonochromatic light are $\Delta\omega/\omega \ll 1$ and $\Delta\lambda\Delta S/\lambda^2 \ll 1$, where ΔS is the largest difference in optical path lengths from the source to the detector, Ref. [16]. The second condition can be translated into the condition that ΔS is small compared to the coherence length of the radiation.

[26] A. VanderLugt, *Optical Signal Processing* (John Wiley & Sons, Inc., New York, 1992). We use slightly different notation than that used in this text.

[27] C. K. Hong, Z. Y. Ou, and L. Mandel, Phys. Rev. Lett. **59**, 566 (1990).

[28] J. Franson, Phys. Rev. A **44**, 4552 (1991).